Title: The generation and characterisation of neutralising antibodies against the Theiler's murine encephalomyelitis virus (TMEV) GDVII capsid reveals the potential binding site of the host cell co-receptor, heparan sulfate

Authors: Nicole Upfold, Caroline Ross, Özlem Tastan Bishop, Garry A. Luke, Caroline Knox

PII: S0168-1702(17)30777-3
DOI: https://doi.org/10.1016/j.virusres.2017.11.017
Reference: VIRUS 97292

To appear in: *Virus Research*

Received date: 10-10-2017
Revised date: 9-11-2017
Accepted date: 15-11-2017

Please cite this article as: Upfold, Nicole, Ross, Caroline, Bishop, Özlem Tastan, Luke, Garry A., Knox, Caroline, The generation and characterisation of neutralising antibodies against the Theiler's murine encephalomyelitis virus (TMEV) GDVII capsid reveals the potential binding site of the host cell co-receptor, heparan sulfate.Virus Research https://doi.org/10.1016/j.virusres.2017.11.017

The generation and characterisation of neutralising antibodies against the Theiler's murine encephalomyelitis virus (TMEV) GDVII capsid reveals the potential binding site of the host cell co-receptor, heparan sulfate

Nicole Upfold[a], Caroline Ross[b], Özlem Tastan Bishop[b], Garry A. Luke[c], Caroline Knox[a*]

[a]Department of Biochemistry and Microbiology, Rhodes University, Grahamstown 6140, South Africa

[b]Research Unit in Bioinformatics (RUBi), Department of Biochemistry and Microbiology, Rhodes University, Grahamstown 6140, South Africa

[c]Centre for Biomolecular Sciences, School of Biology, Biomolecular Sciences Building, University of St Andrews, North Haugh, St Andrews, Scotland KY16 9ST, UK

[*]Correspondence to Caroline Knox; E-mail: caroline.knox@ru.ac.za

Highlights

- TMEV capsid proteins localise to large punctate structures in the cytoplasm during late infection.
- Anti-TMEV capsid antibodies bind a surface loop at the C-terminus of VP1 near the putative receptor binding site.
- Anti-TMEV capsid antibodies neutralise viral infection.
- The TMEV GDVII co-receptor, heparan sulfate, binds to residues in the C-terminal loop of VP1.
- Docking experiments reveal the potential binding site of the co-receptor on the TMEV capsid

Abstract

The early stages of picornavirus capsid assembly and the host factors involved are poorly understood. Since the localisation of viral proteins in infected cells can provide information on

their function, antibodies against purified Theiler's murine encephalomyelitis virus (TMEV) GDVII capsids were generated by immunisation of rabbits. The resultant anti-TMEV capsid antibodies recognised a C-terminal region of VP1 but not VP2 or VP3 by Western analysis. Examination of the sites of TMEV capsid assembly by indirect immunofluorescence and confocal microscopy showed that at 5 hours post infection, capsid signal was diffusely cytoplasmic with strong perinuclear staining and moved into large punctate structures from 6 to 8 hours post infection. A plaque reduction neutralisation assay showed that the anti-TMEV capsid antibodies but not anti-VP1 antibodies could neutralise viral infection *in vitro*. The VP1 C-terminal residues recognised by the anti-TMEV capsid antibodies were mapped to a loop on the capsid surface near to the putative receptor binding pocket. *In silico* docking experiments showed that the known TMEV co-receptor, heparan sulfate, interacts with residues of VP1 in the putative receptor binding pocket, residues of VP3 in the adjacent pit and residues of the adjoining VP1 C-terminal loop which is recognised by the anti-TMEV capsid antibodies. These findings suggest that the anti-TMEV capsid antibodies neutralise virus infection by preventing heparan sulfate from binding to the capsid. The antibodies produced in this study are an important tool for further investigating virus-host cell interactions essential to picornavirus assembly.

Keywords: Theiler's murine encephalomyelitis virus, Neutralising antibodies, Capsid modelling, Surface epitopes, Heparan sulfate, Molecular docking

1. Introduction

The *Picornaviridae* comprises a heterogeneous group of medically and economically important viruses, exemplified by the human and animal pathogens Poliovirus (PV), Enterovirus 71 (EV71), Foot-and-mouth disease virus (FMDV) and Theiler's murine encephalomyelitis virus (TMEV) (Brito et al., 2015; Morales et al., 2016). The picornavirus genome encodes a unique large polyprotein with three functional domains which undergo autoproteolytic cleavage to yield all the viral structural and non-structural proteins necessary for a complete infectious cycle (Jiang et al., 2014). The picornavirus capsid is non-enveloped and composed of 60 copies of four capsid proteins VP1-4 (Stanway, 1990). Assembly begins after cleavage of the P1 precursor into the protein subunits VP0, VP1 and VP3, which immediately assemble into the protomer. Five protomers then combine to form the pentameric subunit of which twelve pentamers interact to

yield the provirion. Finally, cleavage of the VP0 precursor to VP2 and VP4 yields mature infectious virions. (Jiang et al., 2014; Tuthill et al., 2010).

In the mature picornavirus capsid, VP1-3 interact to create the capsid shell and are surface exposed, while VP4 is arranged at the inner surface of the virion. VP1-3 are structurally analogous sharing a wedge-shaped core of eight β-strands. Strand N and C terminal ends are connected by loops that differ in composition and size (Mateu, 1995). Variation in the loop amino acid sequences is responsible for differences in capsid surface topology observed between picornavirus species and serotypes, and also influences receptor binding and antigenicity of the virion, thereby affecting host range, tissue tropism and persistence (Rossmann et al., 2000; Tuthill et al., 2010). The capsid is assembled in a manner that places five VP1 proteins in protruding mesas around the 5-fold axis, and VP2 and VP3 of different protomers in surface protruding heterohexamers on the 3-fold axis (Cathcart et al., 2014). In enterovirus capsids, a deep depression, known as the canyon runs between the mesa and heterohexamer separating surface exposed loops of VP1 from those of VP2 and VP3, while in picornaviruses such as FMDV the depression is reduced or completely absent. In cardiovirus capsids the 5-fold VP1 mesas are star shaped, whose points disrupt the canyon resulting instead in a series of hydrophobic pits (reviewed by Tuthill et al., 2010). Although the precise mechanism of picornavirus capsid assembly is poorly understood, mutational analyses of a small number of picornaviruses including FMDV and the enteroviruses, have identified residues in VP1-3 protein interfaces that are important for capsid function and structure (Ellard et al., 2017; Mateo et al., 2003; Rincón et al., 2015; Ross et al., 2017).

The main purposes of the capsid are to protect the viral genome from environmental conditions and to bind to the host cell to deliver the genome into the cell's interior. Once inside the host's body, enteric viruses attach specifically to a homologous host cell. The initial catch-hold between virus and host cell is mediated through sites on the viral capsid binding to attachment factors on the target cell surface. Picornaviruses exploit a diverse range of host cell receptors for virus attachment and entry, including immunoglobulin superfamily receptors used by PV and cardiovirus encephalomyocarditis virus (EMCV) (Greve et al., 1991; Huber, 1994; Staunton et al., 1989), integrin cell adhesion molecules utilised by FMDV (Monaghan et al., 2005) and decay accelerating factors used by many enteroviruses (Shieh and Bergelson, 2002). Flexibility in

receptor and co-receptor usage has been observed for many species and is often linked to differences in tissue tropism and pathogenesis, for example minor group human rhinoviruses (HRVs) utilise low density lipoprotein receptors (LDLR) while major group HRVs utilise the intercellular adhesion molecule-1 (ICAM-1). Differences in TMEV virulence and tissue-tropism are linked to differences in co-receptor specificity. Neurovirulent strains use heparan sulfate (HS) and persistent strains use α2,3-linked N-acetylneuraminic acid (sialic acid) (reviewed by Tuthill et al., 2010).

Investigations into capsid antigenicity have also shown that immunogenic epitopes on the virus surface can be the target of protective neutralising antibody (nAb) responses in the host (reviewed by Dotzauer and Kraemer, 2012). nAbs play an important role in virus clearance during primary viral infections and in preventing reinfection. Epitopes have been identified on all surface exposed capsid proteins (Meloen Briaire et al., 1983; Westerhuis et al., 2015), however VP1 is the dominant antigenic protein and contains major neutralising epitopes (Cameron et al., 2001; Collen et al., 1991; Edlmayr et al., 2011; Luo et al., 1992; Mateu, 1995; Nitayaphan et al., 1985; Oberste et al., 1999; Wu et al., 2001). Neutralisation sites have been mapped to the N and C termini as well as the EF and GH loops of equine Rhinitis Viruses (ERAV) VP1 (Horsington et al., 2012; Varrasso et al., 2001) and GH loops of FMDV VP1 (Collen et al., 1991). In TMEV, neutralising epitopes have been mapped to the VP1 CD I and II loops as well as the C termini of the protein (Ohara et al., 1988; Tan and Cardosa, 2007; Zurbriggen and Fujinami, 1989) in addition to VP2 EF puff A and B loops (Inoue et al., 1994).

Aspects of picornavirus replication have been well documented while capsid assembly, particularly the early steps from P1 to protomer formation, remains the least understood part of the life cycle. Studies have revealed only the basic steps of capsid oligomerisation, and that pentamers can assemble into empty capsids *in vitro* without assistance from host cell factors and proteins (Li et al., 2012; Rombaut et al., 1991). Evidence suggests that multiple viral and cellular components, such as chaperone proteins of the heat shock family, are required for capsid assembly, particularly the early stages from P1 cleavage to pentamer formation (Geller et al., 2007; Jiang et al., 2014; Macejak and Sarnow, 1992). Few studies have examined the localisation of capsid subunits during infection, and these have largely been restricted to PV or FMDV.

Theiler's murine encephalomyelitis virus (TMEV) is a non-enveloped virus belonging to the *Cardiovirus* genus of the *Picornaviridae*. All TMEV strains produce enteric and neurological diseases in mice and are separated into two subgroups based on their neurovirulence (Lipton, 1980). Theiler's original (TO) subgroup includes the persistent DA and BeAn strains which cause an acute demyelinating illness, similar to multiple sclerosis in humans, while the GDVII and FA strains are highly neurovirulent and induce acute encephalitis (reviewed by Oleszak et al., 2004). A replication system in BHK-21 cells is available and, in this system, we used antibodies against the N-terminal 112 amino acids of VP1 in immunofluorescence experiments to show that the GDVII VP1 protein colocalises with Hsp90 in the cytoplasm and perinuclear region of infected cells (Ross et al., 2016). To extend these studies, antibodies targeting the TMEV capsid proteins (as opposed to VP1 alone) are required, thus rabbits were immunised with purified TMEV GDVII particles. The resultant antibodies were used to investigate the localisation of capsid precursors through the course of TMEV infection. Additionally, the neutralising ability of the antibodies and recognition of linear epitopes near the putative receptor binding site, led to the identification of the potential binding site of the GDVII co-receptor- HS.

2. Materials and Methods

2.1 Cells and virus

BHK-21 cells (kindly provided by M. Ryan, University of St Andrews, UK) were cultured in buffered Dulbecco's modified Eagle Medium (DMEM, Lonza Group Ltd, Basel, Switzerland) supplemented with 5% heat-inactivated foetal calf serum (FCS), 100 U penicillin ml^{-1}, 10 mg streptomycin ml^{-1} and 25 µg fungizone ml^{-1} with 10% CO_2 at 37˚C. The TMEV strain GDVII (GenBank accession no: M20562) was used to infect cells in all experiments. Virus stocks were prepared and titred as described previously (Murray et al., 2009). Cells were infected with virus at a multiplicity of infection (M.O.I) of approximately 3.

2.2 Preparation and purification of TMEV GDVII particles

Cells cultured in four $75cm^2$ flasks grown to 80% confluency were infected with TMEV in serum-free DMEM at a total volume of 2 ml. The virus was allowed to adsorb for 1 h at room temperature (RT) with gentle shaking. 5 ml of serum-free DMEM was added and the flasks were incubated for 24 hours at 37º C to allow for the development of cytopathic effect (CPE), after

which the flasks were frozen at –20º C. To facilitate cell lysis, TMEV infected cells were freeze-thawed three times after which 10% Nonidet P40 (NP-40) (Roche, Germany) was added to a final concentration of 1% and allowed to incubate for 2h at RT, with shaking. Cells were centrifuged at 6 000 x g for 20 minutes using a JA20 rotor (Beckman centrifuge, USA) and 7% polyethylene glycol (PEG MW 6000) (Merck, RSA) and NaCl to a final concentration of 0.38 M were added to the supernatant to concentrate the virus particles, followed by overnight incubation at 4º C. The samples were centrifuged at 11 000 x g at 4º C, for 20 min in Beckman centrifuge tubes using a JA20 rotor. The pellet was resuspended in phosphate buffered saline (PBS) [137 mM NaCl, 2.7 mM KCl, 10 mM Na_2HPO_4, 2 mM KH_2PO_4 (pH 7.4)] and centrifuged on a 30% sucrose cushion at 171 000 x g using a Beckman 70.1Ti rotor (Beckman centrifuge, USA) for 4 h at 4º C. The resultant pellet was resuspended in PBS.

A sucrose gradient was prepared in SW41 tubes (Beckman, USA) with 10% and 40% sucrose, using a gradient master (BioComp, Canada). The pellet obtained from the sucrose cushion was placed at the top of the tube and centrifuged at 96 808 x g using a SW41 rotor (Beckman, USA) for 2 h at 4º C. The resultant virus band was carefully removed using a 7-gauge syringe needle, washed using PBS and centrifuged at 151 263 x g in a SW41 rotor (Beckman, USA) for 1 h at 4º C, and resuspended in 250 µl PBS. 10 µl of the purified virus sample was denatured using 2X loading buffer [100 mM Tris-Cl (pH 6.8), 4% (w/v) sodium dodecyl sulfate (SDS), 0.2% (w/v) bromophenol blue, 20% (w/v) glycerol, 200 mM DTT (diothreitol)] and resolved by 12% SDS-PAGE, and stained with coomassie. Approximately 1 mg of the purified virus sample was used by D. Bellstedt (University of Stellenbosch, South Africa) for the immunisation of rabbits to generate anti-TMEV capsid antibodies (Bellstedt et al., 1987).

2.3 Transmission Electron Microscopy (TEM)

Purified virus was prepared for TEM according Lipton and Friedmann (1980) except that sodium phosphotungstate was replaced with a 3% solution of uranyl acetate. Grids were viewed using a Carl Zeiss Libra 120 PLUS transmission electron microscope and ITEM software was used to capture the images (Carl Zeiss, Germany).

2.4 Preparation of infected cell lysate and Western blot

To produce infected cell lysates, 75 cm^2 flasks containing BHK-21 cells were infected with TMEV in serum-free DMEM. Following a virus adsorption period of 1 h, at RT with shaking, virus inoculum was aspirated and the cells rinsed twice with PBS before 5 ml DMEM was added. The cells were incubated at 37°C, and harvested at various hours post infection (hpi). Control cells were mock-infected with serum-free DMEM. Cells were collected following treatment with trypsin and centrifugation at 1000 x g and were resuspended in PBS. For Western analysis experiments, total proteins were denatured in 2X SDS loading buffer and resolved by 12% SDS-PAGE. Proteins were transferred onto nitrocellulose membrane (Bio-Rad, USA) before probing with the anti-TMEV capsid antibodies. Detection was performed using the BM Chemiluminescence Western Blotting Kit (Roche, Mannheim, Germany) according to the manufacturer's instructions. Protein bands were visualised using the ChemiDoc Molecular Imager XRS^+ (Bio-Rad, USA), and image analysis was performed using the Image Lab™ software, version 5.1.

2.5 Plasmids

Plasmids containing the TMEV VP1 full length protein and VP1 truncations were constructed. The sequence of TMEV VP1 was obtained by PCR of pGDVIIFL2, a plasmid that carries the full-length cDNA of TMEV GDVII (Fu et al., 1990), using the KAPA Taq ReadyMix kit (KAPA Biosystems, South Africa). The forward primer NUVP1F and reverse primers NUVP1R, NU1-112R, NU1-195R and NU1-221R were used to generate the plasmids pVP1 (Full length), pVP1$\Delta_{113\text{-}276}$, pVP1$\Delta_{196\text{-}276}$, pVP1$\Delta_{222\text{-}276}$ (C-terminal truncations) respectively. Primers NU159-276F and NU159-276R were used to generate pVP1$\Delta_{1\text{-}158}$ (N-terminal truncation) (Table 1). PCR cycles included an initial denaturation step at 95º C for 1 min, 30 cycles of: denaturation at 95º C for 1 min, annealing at 60º C for 1 min and elongation at 72º C for 1 min, followed by a final elongation step at 72º C for 7 min. The PCR products were ligated into the plasmid vector pQE-80L (Qiagen, Mannheim, Germany) by restriction with *BamHI* and *SalI* (ThermoFischer Scientific, USA). To confirm the presence of the inserts and correct open reading frames, all plasmids were sequenced by Inqaba Biotechnical Industries (Pty) Ltd., Pretoria South Africa.

2.6 Protein expression, and analysis

E. coli JM109 cells transformed with pQE-80L, pVP1, pVP1$\Delta_{113\text{-}276}$, pVP1$\Delta_{196\text{-}276}$, pVP1$\Delta_{222\text{-}276}$ and pVP1$\Delta_{1\text{-}158}$ were cultured in Luria broth (LB) supplemented with 100 µg/ml ampicillin

overnight at 37°C. Cultures were induced with 1 mM Isopropyl β-D-1-thiogalactopyranoside (IPTG) for 4 h and duplicate samples collected each hour. Centrifugation at 11,800 x g was used to pellet the cells which were resuspended to equivalent density in PBS. Proteins were denatured using 2X loading buffer and resolved by 12% SDS-PAGE before being transferred onto nitrocellulose membrane for Western blotting using Anti-His6(2) antibodies (Roche, Germany), recognising the 6X histidine tag in pQE-80L, at a dilution of 1:3000. Anti-TMEV capsid antibodies were used at a dilution of 1: 20 000.

2.7 Indirect immunofluorescence and confocal microscopy

BHK-21 cells grown on sterile 13 mm glass coverslips in six-well plates were washed twice with serum-free DMEM before 1:1 TMEV GDVII virus stock: serum-free DMEM (2 ml total volume) was added to each well. Following a virus adsorption period of 1 h, at RT with shaking, virus inoculum was aspirated and the cells rinsed twice with PBS before 5 ml DMEM was added. The cells were incubated at 37°C, and fixed at various hpi. Control cells were mock-infected with serum-free DMEM. Cells were washed with PBS before fixation with 4% paraformaldehyde for 20 min at RT, then rinsed twice with PBS. For staining, cells were permeabilised in PB (10% sucrose, 0.1% Triton X-100 in PBS) for 20 min, blocked in PB containing 2% BSA (Block) for 40 min at RT and incubated with antibodies against TMEV GDVII 2C (1:1000) (Jauka et al., 2010), anti-TMEV VP1 antibodies (1: 20 000) (Ross et al., 2016) or anti-TMEV capsid antibodies (1:20 000), diluted in block buffer for 1 h with shaking. Cells were washed twice in PBS containing 0.1% Tween-20 and incubated with species-specific Alexa Fluor 546 or 488-conjugated secondary antibodies (Invitrogen, USA) (1:500) for 30 min. Cells were washed three times, and 4',6-diamino-2-phenylindole dihydrochloride (DAPI, Sigma, St Louis, USA) was added at a final concentration of 0.8 µg/ml in the second wash step to stain the nucleus. The slides were mounted using Dakofluorescence mounting medium (Dako Inc., CA, USA) and stored at RT. The helium/neon and argon lasers at wavelengths 405, 488 and 543 nm were used to excite, DAPI, Alexa Fluor 488 and Alexa Fluor 546 respectively. Images were captured using the Zeiss LSM 510-Meta laser scanning confocal microscope and analysed using Zen software (2012 blue edition, Zeiss, Germany). To acquire a representative image for each experiment, over 50 cells were viewed at 63 x magnification. Immunofluorescence experiments were performed in triplicate.

2.8 Antibody neutralisation assay

The abilities of anti-TMEV capsid and anti-TMEV VP1 (Ross et al., 2016) antibodies to neutralise virus infection *in vitro* were assessed by measuring the inhibition of viral plaque formation using a plaque reduction neutralisation assay. Antibodies were diluted to 1:50, 1:100, 1:500 and 1:1000 in serum-free DMEM. TMEV stocks were diluted in serum-free DMEM to 10^{-4}. Equal volumes of virus and serum dilutions were added, giving a final virus dilution of $5x10^{-5}$ and serum dilutions of 1:100, 1:200, 1:1000 and 1:2000 (in a total volume of 300 µl), and were left to co-incubate with gentle agitation for 1.5 hours at 37º C. Virus-serum mixtures were then added to confluent BHK-21 monolayers in 6 well plates, to adsorb for 30 min at RT with gentle agitation and then 2.5 hours at 37º C. The cells were washed with PBS, overlayed with 3ml of overlay solution (50% DMEM, 1.25% methocel, 60mM NaCl) and incubated at 37º C until visible plaques were observed. Cells were washed and fixed in 4% paraformaldehyde for 15 min at RT then stained with Coomassie Brilliant Blue. The number of plaques for each well was counted. Pre-immune serum (final dilution of 1:100) and mock-infected controls were used. All experiments were performed in triplicate.

2.9 In silico virus structure assembly

A homology model of the TMEV GDVII protomer was obtained from a previous study (Ross et al., 2016). The model did not contain water molecules or bound ligands. The protomer complex was solvated and minimised using GROMACS 5.1.2 (Abraham et al., 2015). The complex was subjected to 1700 steps of steepest descent energy minimisation. A complete viral capsid was then assembled by superimposing 60 copies of the minimised protomer on the biological assembly of a template virus (TMEV DA strain; PDB ID: 1TME) (Grant et al., 1992). It is thought that the host cell receptor of TMEV is situated in a hydrophobic pit that is located near the interface between two adjacent protomers around the five-fold axis. This receptor binding region is the focus of interest for the docking of the co-receptor HS and can be investigated by locally analysing any one of the 60 pits within the capsid. Therefore, to lower the computational cost of the docking studies, a second complex comprising of only two adjacent protomers was also assembled. This complex is termed the protomer interface complex.

2.10 Epitope mapping

Two respective epitope regions were mapped to the assembled TMEV GDVII virus capsid. These regions were VP1 (1-112) and VP1 (222-276). To identify which epitope regions were located on the surface, the virus capsid was visualised in PyMol (Schrodinger, 2010). In addition to exploring the location of epitope regions, the suggested HS binding motif (Reddi and Lipton, 2002) YKKMKV, located in VP1 (240-245), was also mapped to the capsid model.

2.11 Molecular docking

Sialic acid and HS compounds were retrieved from the ZINC database (Irwin and Shoichet, 2005). The two compounds were individually docked to the protomer interface complex using AutoDock4.2 (Morris et al., 2010). AutoDock Tools (ADT) were used to prepare the protomer interface complex and the ligands. The partial charges of the ligands were assigned using the Gasteiger-Hückel algorithm. Sialic acid binds to the capsid in a pit located between VP1 loop II and VP2 Puff B (Tsunoda et al., 2010). Therefore, for sialic acid the grid box was centred on this pit and spanned an area of residues around a 15 Å radius. The binding site of HS is unknown. To identify the potential binding site of HS, four docking simulations were performed. For each simulation, a grid box spanning a 35 Å radius was centred on a different region across the protomer interface complex. All docking simulations were carried using the Lamarckian Genetic Algorithm (LGA) with the following parameters: population size of 300, 100 LGA runs, a maximum of 250,000 energy evaluations and a maximum of 27,000 generations. LigPlot+ (Laskowski and Swindells, 2011) was used to determine the residue interactions between the protomer interface complex and ligands that docked with the lowest binding energy.

3. Results

3.1 Sucrose gradient purification of TMEV GDVII infected cells yields pure intact virus particles

To produce polyclonal antibodies against TMEV GDVII capsids, BHK-21 cells were infected with TMEV GDVII for 24 hours and the virus particles were purified using a 30% sucrose cushion and 10-40% sucrose gradient. Transmission electron micrographs (Fig. 1A panels a and b) showed the presence of numerous virus particles roughly 31 nm in diameter with icosahedral symmetry. Particles that appeared to be damaged or empty (yellow arrowheads) were also present in the sample, but were not abundant (Fig. 1A panel b). SDS-PAGE analysis of

denatured capsid samples resolved bands for three proteins at the expected sizes of 37kDa, 34kDa and 27kDa for TMEV VP1, VP2 and VP3 respectively (Fig. 1B).

3.2 Anti-TMEV capsid antibodies detect VP1 but not VP2, VP3 or VP4 by Western analysis

To determine whether the anti-TMEV capsid antibodies could detect viral capsid proteins in infected cell lysates, BHK-21 cells were infected or mock infected with TMEV for a period of 8 hours. Cells were collected at hourly intervals and total cell lysates were analysed by Western blot. A single protein band of approximately 37kDa corresponding to VP1 was detected from 5 hpi in infected cells, and signal increased in intensity as time progressed to 8 hpi (Fig. 2A). No bands were detected in mock-infected cell lysate and pre-immune serum could not detect protein bands in infected or mock infected cell lysates indicating that the antibodies were recognising viral protein.

3.3 Anti-TMEV capsid antibodies recognise linear epitopes in the C-terminal region of VP1

To define the region of amino acid residues in VP1 recognised by anti-TMEV capsid antibodies during Western blot experiments, a deletion analysis was performed on the VP1 protein. The full-length VP1 coding sequence and C- or N-terminally truncated coding sequences were PCR amplified and cloned into pQE-80L (Fig. 2B). Once transformed, expression was induced for 4 hours following the addition of IPTG. Whole cell lysates were used in Western blot experiments using Anti-His6(2) antibodies to confirm that the expression of each protein was successful (data not shown). Anti-TMEV capsid antibodies could detect full-length VP1 as expected (Fig. 2C). The anti-TMEV capsid antibodies were not able to recognise the VP1 C-terminal truncates VP1$\Delta_{113\text{-}276}$, VP1$\Delta_{196\text{-}276}$ or VP1$\Delta_{222\text{-}276}$, but were able to detect the N-terminal truncate VP1$\Delta_{1\text{-}158}$, mapping the binding region to 54 amino acids 222-276 in the C-terminus of VP1. The anti-TMEV capsid antibodies were not able to detect the empty pQE-80L vector, as expected (Fig. 2C).

3.4 TMEV capsid proteins localise to the cytoplasm of infected cells forming punctate structures towards the end of infection

To examine the subcellular distribution of TMEV capsid precursors through the course of infection BHK-21 cells were infected or mock infected with TMEV, fixed with 4% paraformaldehyde at 4, 5, 6, 7 and 8 hpi, and probed with anti-TMEV capsid antibodies. No

capsid signal was detected in mock infected cells (Fig. 3 panel a) or in TMEV infected cells stained with secondary antibodies alone (Fig. 3 panel b). To confirm that cells were successfully infected with TMEV, cells were stained with anti-TMEV VP1 specific and anti-TMEV 2C antibodies (Fig. 3 panels c and d). Signal for VP1 was cytoplasmic with increased signal intensity in the perinuclear region as expected (Ross et al., 2016), while 2C was apparent in the perinuclear replication complex as previously reported (Jauka et al., 2010; Murray et al., 2009). Following optimisation of anti-TMEV capsid antibodies, a dilution of 1: 20 000 was found to accurately detect capsid signal without non-specific staining (data not shown). No signal was observed for TMEV capsid proteins in cells at 4 hpi (Fig. 3 panel e), however a bright signal was detected from 5 hpi, and was diffusely cytoplasmic, but dominant in the perinuclear region of the cell (Fig. 3 panel f). The distribution of TMEV capsid protein changed dramatically from 6 to 8 hpi where the signal moved progressively into large punctate structures within the cell cytoplasm (Fig. 3 panels g-i). TMEV capsid proteins remained absent from the nucleus at all time-points post infection. The same distributions were observed in all infected cells at respective timepoints, in three independent experiments.

3.5 Anti-TMEV capsid antibodies but not anti-TMEV VP1 antibodies neutralise TMEV infection

To determine whether the anti-TMEV capsid and previously produced anti-TMEV VP1 antibodies (Ross et al., 2016) were able to neutralise *in vitro* viral infection, increasing concentrations of sera were incubated with TMEV virus at a dilution of $5x10^{-5}$, before the residual viral infectivity was measured by plaque assay on BHK-21 monolayers. The results indicate that as concentrations of anti-TMEV capsid containing serum increase, TME viral plaque formation decreases dramatically. Sera produced against the N-terminal region of TMEV VP1 does not neutralise TME virus infection at any concentration (Fig. 4, A and B). Anti-capsid serum at a dilution of 1: 2000 inhibited plaque formation ~5-fold, and up to ~120-fold at a dilution of 1:100 (Fig. 4B).

3.6 C-terminal residues 254-274 *reside on a surface exposed loop*

The epitope regions detected by the anti-TMEV capsid and anti-TMEV VP1 antibodies were mapped to the TMEV GDVII capsid. It is clear that the anti-TMEV VP1 antibodies previously generated against a peptide spanning the region VP1 (1-112) recognise regions within the N-terminal (1-112) amino acids of the protein. Epitopes recognised by polyclonal antibodies

generated against a mature virus particle however, may be situated anywhere on the capsid surface. The deletion analysis revealed that the anti-TMEV capsid antibodies bind linear epitopes located within the region VP1 (222-276). It is likely that the two sets of antibodies recognise areas in (1-112) and (222-276) that are exposed on the virus surface, therefore we explored the structural locations of VP1 (1-112) and VP1 (222-276). The structural mapping of the TMEV GDVII capsid is shown in Fig. 5. Within the VP1 (1-112) peptide, three regions are exposed on the surface (47-57), (79-87) and (95-112). The regions are adjacent to each other and form a larger area that extends towards the interface between the VP1, VP2 and VP3 subunits (Fig. 5B). The (95-112) region contains VP1 loop II (98-105). This loop is clearly indicated in the cartoon depiction (Fig. 5C) and neighbours the VP2 Puff B loop. With regard to VP1 (222-276), the residues 254-274 are located on the surface of the capsid. These residues form a loop in the C-terminus of VP1 at the VP1-VP3 interface (Fig. 5A-C).

3.7 The TMEV host cell co-receptor, heparan sulfate, is predicted to bind to a pit at the VP1-VP3 interface below the VP1 C-terminal loop

Two co-receptors, sialic acid and HS, were docked to a complex comprising of two adjacent protomers from the GDVII capsid model. The binding site of sialic acid has been previously identified as a pit located between VP1 loop II and VP2 Puff B (Zhou et al., 2000). In this study, a targeted docking of sialic acid was performed as a control for docking experiments. The pit between VP1 loop II and VP2 Puff B marked the centre of a grid box that spanned a 15 Å radius. The docking results were consistent with previous studies and indicated that sialic acid has a high binding affinity to this pit. From a total of 100 LGA runs (Supplementary Table S1), the best docked conformation had a binding energy of -5.88. The results of the LigPlot analysis (Fig. 6A panel a) indicate the predicted residue interactions between the docked sialic acid compound and the viral capsid. As predicted sialic acid binds to residues of VP1 loop II through electrostatic interactions with R97, S98, G99, G100 and A104. This loop forms part of the surface exposed region recognised by the antibodies generated against the peptide VP1 (1-112).

The binding site for HS is unknown, but VP1 (240-YKKMKV-245) is thought to be a possible HS binding motif (Reddi and Lipton, 2002). To explore this further the motif was mapped to the viral capsid. The motif is in fact buried deep within the viral capsid and is not surface exposed, as such it is unlikely to be the binding site of HS (Fig. 6B). To explore all possible binding sites

across the protomer, a series of four docking simulations were performed, such that in each simulation the grid box was centred on a different region of the protomer complex. In addition, a larger grid box spanning a 35 Å radius was defined for each simulation. Out of the four docking simulations, only one revealed high affinity binding for HS to the viral capsid. Specifically, significant docking results were only observed when the grid box was centred on the VP1 residue L252, situated in a pit directly below the VP1 C-terminus loop (254-274) and neighbours the VP1 hydrophobic pocket at the VP1-VP3 interface, the suggested binding site of the host cell receptor. HS docked directly into this pit with a lowest energy conformation of -8.58 (Supplementary Table S2). The residue interactions between HS and the capsid subunits (Fig. 6A panel b) depict multiple electrostatic and covalent bonds with VP1 and VP3 residues. Notably, HS docked around a central VP1 residue F254 that is located in the C-terminus loop recognised by the anti-TMEV capsid antibodies. The molecule also interacts with the P257 residue in the C-terminus loop and with VP1 P153, A154, D155 residues that form part of the hydrophobic pit in the adjacent protomer. HS also interacts with VP3 T174, S175, Y176, which are located within the pocket of the local protomer. Ligands bound to the capsid surface are depicted in Fig. 6C.

4. Discussion

The main aim of this study was to generate polyclonal antibodies against the TMEV GDVII capsid proteins and characterise their antigen recognition properties as well as neutralisation ability during TMEV infection. The antibodies detected the linearised 37 kDa TMEV VP1 protein when purified virus and infected cell lysates were analysed by Western blotting. It was anticipated that antibodies targeting VP1 epitopes would be present in the serum, as VP1 is the most surface exposed and immunodominant of the capsid proteins (Edlmayr et al., 2011; Meloen Briaire et al., 1983; Rossmann et al., 1985). Linear epitopes have also been reported for TMEV VP2 and VP3 (Inoue et al., 1994; Kim et al., 1992). The inability to detect these linearised epitopes is therefore unexpected, but is possibly due to low concentrations of specific antibodies or the presence of conformational epitopes in the mature capsid. VP4 is the smallest capsid protein at 6 kDa and is arranged internally in the capsid particle (Jiang et al., 2014; Stanway, 1990), thus the absence of antibodies to linear epitopes in VP4 is not surprising.

The next experiments investigated the antibody recognition site on VP1. Linear epitopes have been identified within the VP1 proteins of many picornaviruses including duck hepatitis A virus

(DHAV) (Wu et al., 2015), enterovirus 71 (EV71) (Zhang et al., 2012) and FMDV (Yang et al., 2011). In TMEV, epitopes have been identified around amino acid 101 in DA VP1 (Zurbriggen et al., 1989) and at positions 12-25, 145-160, 262-276 in BeAn VP1 (Inoue et al., 1994). We previously identified five major surface accessible epitopes in the N-terminal 1-112 amino acids of VP1 using an *in-silico* analysis, and produced responding antibodies against a peptide encoding this N-terminal region (Ross et al., 2016). We therefore tested whether the anti-TMEV capsid antibodies would detect epitopes in this highly antigenic region by performing a deletion analysis of the VP1 protein. The anti-TMEV capsid antibodies could not recognise linear epitopes within the N-terminal half of VP1, but instead recognised a truncated protein consisting of C-terminal amino acids 159-276. The *in-silico* analysis presented by Ross et al (2016) also identified epitopes in the C-terminal amino acids 251-276 of VP1, which are likely those that elicited the production of the anti-TMEV capsid antibodies.

To investigate the localisation of capsid precursors through a time-course of infection, TMEV infected BHK-21 cells were fixed using 4% paraformaldehyde from 4-8 hpi and probed with anti-TMEV capsid antibodies. A clear signal was detected from 5 hpi in infected cells but not in mock infected cells, indicating that the antibodies were specific for capsid proteins. At 5 hpi the anti-TMEV capsid signal was diffusely cytoplasmic, with increased signal in the perinuclear region, but was absent from the nucleus. Similar cytoplasmic localisation patterns have been observed for the VP1 proteins of FMDV (Knox et al., 2005), PV (Wychowski et al., 1985) and TMEV GDVII (Ross et al., 2016) and DA (Nedellec et al., 1998), as well as the VP0, VP1 and VP3 proteins of EV71 (Liu et al., 2013).

Interestingly, from 6 hpi, the capsid signal changed from a diffuse cytoplasmic pattern into distinct punctate structures which were most prominent at 8 hpi and resembled those observed by Nedellec and colleagues (1998) for TMEV GDVII at 5 hpi. These punctate structures are possibly intracytoplasmic crystalline arrays formed by the accumulation of viral capsids prior to host cell death, first observed by Friedmann and Lipton, (1980). Whether these structures are sites of capsid assembly and membrane associated is yet to be determined although our preliminary data suggests that they do not colocalise with membranes of the distal secretory pathway (not shown).

Previous studies investigating localisation of viral capsids have involved the use of antibodies targeting the individual capsid proteins as opposed to antibodies generated against whole capsid (Liu et al., 2013, Knox et al., 2005, Nedellec et al., 1998 and Ross et al., 2016). Whether the anti-TMEV capsid antibodies in this study recognise individual capsid proteins, a subset thereof, or epitopes on assembled capsid precursors isnot known. Although evidence suggests that the individual capsid proteins are never separate in the cell but rather assemble immediately into the protomer following cleavage of P1 (Bruneau et al., 1983), the anti-TMEV antibodies were able to detect VP1 and VP3 but not VP2 when expressed as GFP tagged proteins by immunofluorescence (data not shown). These results suggest that the antibodies possibly recognise conformational epitopes on these proteins that are present in the mature capsid. Additionally, it is unlikely that the anti-capsid antibodies recognised the immature VP0 precursor, as it is proteolytically cleaved to the VP2 and VP4 proteins in the mature capsid.

Protective nAbs targeting the surface exposed capsid proteins have been identified for many picornavirus species including the VP1 and VP2 proteins of TMEV (Cameron et al., 2001; Inoue et al., 1994; Kim et al., 1992). Since the anti-TMEV capsid antibodies in this study and anti-TMEV VP1 antibodies (Ross et al., 2016) recognised linear epitopes within in the C-terminal and N-terminal regions of VP1 respectively, the next experiments examined the *in vitro* neutralising abilities of the two sets of antibodies. Plaque reduction neutralisation assays demonstrated that the anti-TMEV VP1 antibodies could not neutralise viral infection, whereas anti-TMEV capsid antibodies were able to reduce the number of plaques by ~120-fold when diluted 1:100. Investigations into the antigenicity of TMEV VP1 have identified nAbs targeting only the C-terminal region of the protein and not the N-terminus. For example, Inoue et al., (1994) reported three predominant linear epitopes in BeAn VP1, namely VP1(12-25), VP1(146-160) and VP1(262-276) with only VP1(262-276) eliciting nAbs. Furthermore, it is possible that the anti-TMEV capsid antibodies detect the same VP1(262-276) epitope in GDVII, as amino acid sequences between the two strains are highly conserved for this region (data not shown).

Epitopes must be surface exposed to be detected on the mature capsid particle. Many of the VP1 N-terminal residues described in Ross et al., (2016) were predicted to be surface exposed in the protomer, but their location in the mature virus particle was not investigated. Since we observed that C-terminal but not N-terminal VP1 epitopes elicited neutralising antibodies, amino acids 1-

112 and 222-276 were mapped to the capsid surface to better understand their locations. Amino acid residues 47-57, 79-87 and 95-112 were found to be situated near the VP1-VP3 interface, with residues 98-105 forming VP1 loop II next to VP2 Puff B. Residues 254-274 were found to form a large flexible loop at the VP1-VP3 interface. The position of residues 254-274 and their detection by anti-TMEV capsid antibodies is consistent with multiple studies that demonstrate that the highly variable loops at the virion surface are the most exposed residues of the capsid, and typically contain neutralising epitopes (Luo et al., 1992; Mateu, 1995; Rossmann et al., 1985). Additionally, this loop protrudes over the lateral extension of a pit believed to be the binding site for the host cell receptor in DA and BeAn strains (Grant et al., 1992; Luo et al., 1992).

Host cell receptors have been identified for a number of picornaviruses (reviewed by Tuthill et al., 2010). Several investigations have failed to identify the TMEV host cell receptor but suggest that both persistent and virulent strains of the virus bind to an unknown 37 kDa glycoprotein (Kilpatrick and Lipton, 1991). Co-receptors are thought to assist with host cell receptor binding and different molecules have been identified as co-receptors for the different TMEV subgroups. Persistent strains use the N-linked glycoprotein sialic acid as a receptor moiety (Fotiadis et al., 1991; Shah and Lipton, 2002) while highly-neurovirulent strains use HS, a proteoglycan (Reddi and Lipton, 2002). HS typically recognises and binds to heparin-binding domains (HBD) which consist of basic amino acids separated by hydrophobic residues (Cardin and Weintraub, 1989). A potential HBD in the VP1 C-terminus (YKKMKV) identified by Reddi and Lipton (2002) was mapped to the full capsid and is unlikely to be the HS binding site as it is found at positions 240-245 which are buried deep within the viral capsid. *In silico* docking experiments were therefore used to determine the residues that HS likely binds and these results were used to map HS bound to the full capsid structure. The results showed that HS interacts with residues in the hydrophobic pit situated at the VP1-VP3 interface which is thought to be the host cell receptor binding site (Luo et al., 1992). Furthermore, HS also interacts with residues in a pocket below and residues of the C-terminal loop recognised by the neutralising anti-TMEV capsid antibodies produced in this study. Taken together the results suggest that the binding of anti-TMEV capsid neutralising antibodies to the C-terminal loop hinders HS binding and therefore receptor binding, preventing viral attachment and entry.

In conclusion, this study generated neutralising anti-TMEV capsid antibodies that not only detected viral protein in infected cells but also revealed a potential binding site for the TMEV GDVII co-receptor, HS. These antibodies provide a valuable tool with which to further investigate the host cell interactions that govern the capsid assembly process.

Acknowledgements

The authors gratefully acknowledge H. Lipton for providing TMEV GDVII cDNA, and D. Lang for assistance with the confocal analysis. This work was supported by Medical Research Council (MRC, South Africa) and Research Council (RC, Rhodes University) grants. CR and ÖTB thank the National Research Foundation of South Africa (grant number 93690). NU was supported by postgraduate fellowships from the NRF and the German Academic Exchange Service (DAAD) and a Henderson Fellowship from Rhodes University. The content of this publication is solely the responsibility of the authors and does not necessarily represent official views of the funders.

Fig. 1. TMEV GDVII virus particles purified from infected BHK-21 cells by sucrose cushion and sucrose gradient purification. (A) TEM of GDVII virus particles following sucrose cushion (top panel) and sucrose gradient (bottom panel) purification. Yellow arrows indicate intact empty capsids. (B) Presence of capsid proteins confirmed by 12% SDS-PAGE analysis, following sucrose gradient purification. Mw (Molecular weight marker in kDa).

Fig. 2. Detection of TMEV GDVII VP1 in infected BHK-21 and bacterial lysates and mapping of linear antigenic regions in VP1. (A) Western analysis of TMEV infected BHK-21 lysates at various times post-infection, using anti-TMEV capsid antibodies. MW (molecular weight marker in kDa). (B) The strategy used to generate truncated VP1 his-fusion proteins. The red boxes represent the his-coding sequence. The blue boxes represent the truncated regions of VP1. The numbers above the boxes represent the nucleotide locations. Numbers following Δ denote the deleted amino acids. Dashed lines represent the region recognised by anti-capsid antibodies. (C) Western Blot of bacterially expressed lysates. Cells were transformed with plasmid constructs and induced for 4 h using IPTG. Whole cell lysates were analysed by Western blot using anti-TMEV capsid antibodies to determine the regions of VP1 detected by the antibodies. MW (molecular weight marker in kDa)

Fig. 3. Subcellular distribution of TMEV capsid proteins in infected BHK-21 cells. Cells were mock infected (panel a), or infected with TMEV (panels b-i), fixed with 4% paraformaldehyde at 4-8 hpi and stained with anti-TMEV VP1 (5 hpi) (panel c), anti-TMEV 2C (4hpi) (panel d) or anti-TMEV capsid antibodies (4-8 hpi) (panels e-i). Primary antibodies were detected using species specific Alexa Fluor 488-conjugated or 546-conjugated secondary antibodies. Cells in panel b were probed with secondary 488-conjugated antibodies only. Scale bars = 20μm.

Fig. 4. *In vitro* neutralising abilities of polyclonal anti-TMEV capsid and anti-TMEV VP1 antibodies. (A) A representative result of three independent experiments for each treatment. (B) Quantitative comparison of the neutralising activities of anti-TMEV capsid and anti-TMEV VP1 antibodies at increasing concentrations of sera. 100% confluent BHK-21 cells were infected with TMEV pre-incubated with increasing concentrations of anti-TMEV capsid and anti-TMEV VP1 sera. After removal of virus-serum inoculum, neutralising ability was analysed by plaque reduction assay. Neutralising ability is expressed as the decrease in plaque number with

increasing serum concentration. Pre-immune sera were used as controls for each treatment, at a dilution of 1:100. All experiments were repeated in triplicate. Error bars show standard deviation of the mean.

Fig. 5. Structural mapping of the TMEV GDVII capsid. (A) Homology model of a mature TMEV GDVII capsid. Subunits are coloured as: Green-VP1; Pink-VP2; Orange-VP3. Surface exposed residues of VP1 N-terminal (1-112) containing linear epitopes detected by the anti-TMEV VP1 antibodies (Ross et al., 2016): Blue-VP1 residues 47-57, 79-87 and 95-112. Surface exposed residues of VP1 C-terminal (222-276) containing linear epitopes detected by the anti-TMEV capsid antibodies: Black-VP1 residues 254-274. (B) Local region showing surface of the virus. (C) Cartoon depiction of the local capsid region that contains the predicted surface exposed linear epitopes.

Fig. 6. Residue interactions of TMEV GDVII capsid with sialic acid and heparan sulfate. (A) Residue interactions between the capsid proteins VP1 and VP2 with sialic acid (left panel), and the capsid proteins VP1 and VP3 with heparan sulfate (right panel). Residues from an adjacent protomer are indicated with italic blue labels. The figures were generated in LigPlot, subsequent to AutoDock docking simulations. (B) Cross-section through the capsid surface. The motif VP1 240-YKKMKV-245 (predicted by Reddi and Lipton, 2002) is mapped in purple (circled in black) and lies deep beneath the surface of the capsid. (C) Local region showing docked co-receptors on the surface of the virus. Docked co-receptors are coloured as: Yellow-sialic acid; Red-heparan sulfate. The hydrophobic pocket is indicated by a white circle, VP1 C-terminal residues 222-276 are coloured in Black, VP1 residues 47-57, 79-87 and 95-112 are coloured in Blue.

References

Abraham, J.M., Murtola, T., Schulz, R., Pall, S., Smith, J.C., Hess, B., Lindahl, E., 2015. GROMACS : High performance molecular simulations through multi-level parallelism from laptops to supercomputers. SoftwareX 1–2, 19–25. doi:10.1016/j.softx.2015.06.001

Bellstedt, D.U., Human, P.A., Rowland, G.F., Van der Merwe, K.J., 1987. Acid-treated, naked bacteria as immune carriers for protein antigens. J. Immunol. Methods 98, 249–255. doi:10.1016/0022-1759(87)90012-3

Brito, B.P., Rodriguez, L.L., Hammond, J.M., Pinto, J., Perez, a. M., 2015. Review of the Global Distribution of Foot-and-Mouth Disease Virus from 2007 to 2014. Transbound. Emerg. Dis. n/a-n/a. doi:10.1111/tbed.12373

Bruneau, P., Blondel, B., Crainic, R., Horodniceanu, F., Girard, M., 1983. Poliovirus Type 1 Capsid Polypeptides: Absense of a Free Form In The Cytoplasm of Iinfected HeLa Cells. Ann. Virol. 134, 151–164.

Cameron, K., Zhang, X., Seal, B., Rodriguez, M., Njenga, M.K., 2001. Antigens to viral capsid and non-capsid proteins are present in brain tissues and antibodies in sera of Theiler's virus-infected mice. J. Virol. Methods 91, 11–19. doi:10.1016/S0166-0934(00)00246-9

Cardin, A.D., Weintraub, H.J.R., 1989. Molecular Modeling of Protein-Glycosaminoglycan Interactions. Arterioscler. Thromb. Vasc. Biol. 9, 21–32. doi:doi: 10.1161/01.ATV.9.1.21

Cathcart, A.L., Baggs, E.L., Semler, B.L., 2014. Picornaviruses: Pathogenesis and Molecular Biology, 3rd editio. ed, Reference Module in Biomedical Research. Elsevier. doi:10.1016/B978-0-12-801238-3.00272-5

Collen, T., Dimarchi, R., Doel, T.R., 1991. A T cell epitope in VP1 of foot-and-mouth disease virus is immunodominant for vaccinated cattle. J. Immunol. 146, 749–755.

Dotzauer, A., Kraemer, L., 2012. Innate and adaptive immune responses against picornaviruses and their counteractions: An overview. World J. Virol. 1, 91–107. doi:10.5501/wjv.v1.i3.91

Edlmayr, J., Niespodziana, K., Popow-Kraupp, T., Krzyzanek, V., Focke-Tejkl, M., Blaas, D.,

Grote, M., Valenta, R., 2011. Antibodies induced with recombinant VP1 from human rhinovirus exhibit cross-neutralisation. Eur. Respir. J. 37, 44–52. doi:10.1183/09031936.00149109

Ellard, F.M., Drew, J., Blakemore, W.E., Stuart, D.I., King, A.M.Q., 2017. Evidence for the role of His-142 of protein 1C in the acid- induced disassembly of foot-and-mouth disease virus capsids 1911–1918.

Fotiadis, C., Kilpatrick, D.R., Lipton, H.L., 1991. Comparison of the binding characteristics to BHK-21 cells of viruses representing the two Theiler's virus neurovirulence groups. Virology 182, 365–370.

Friedmann, A., Lipton, H.L., 1980. Replication of Theiler's murine encephalomyelitis viruses in BHK21 cells: An electron microscopic study. Virology 101, 389–398. doi:10.1016/0042-6822(80)90452-3

Fu, J., Stein, S., Rosenstein, L., Bodwell, T., Routbort, M., Semler, B.L., Roos, R.P., 1990. Neurovirulence Determinants of genetically engineered determinants Neurovirulence Theiler viruses. Proc. Natl. Acad. Sci. U. S. A. 87, 4125–4129.

Geller, R., Vignuzzi, M., Andino, R., Frydman, J., 2007. Evolutionary constraints on chaperone-mediated folding provide an antiviral approach refractory to development of drug resistance. Genes Dev. 21, 195–205. doi:10.1101/gad.1505307

Grant, R. a, Filman, D.J., Fujinami, R.S., Icenogle, J.P., Hogle, J.M., 1992. Three-dimensional structure of Theiler virus. Proc. Natl. Acad. Sci. U. S. A. 89, 2061–2065. doi:10.1073/pnas.89.6.2061

Greve, J.M., Forte, C.P., Marlor, C.W., Meyer, A.M., Hoover-Litty, H., Wunderlich, D., McClelland, A., 1991. Mechanisms of receptor-mediated rhinovirus neutralization defined by two soluble forms of ICAM-1. J. Virol. 65, 6015–23.

Horsington, J.J., Gilkerson, J.R., Hartley, C.A., 2012. Mapping B-cell epitopes in equine rhinitis B viruses and identification of a neutralising site in the VP1 C-terminus. Vet. Microbiol. 155, 128–136. doi:10.1016/j.vetmic.2011.08.022

Huber, S.A., 1994. VCAM-1 is a receptor for encephalomyocarditis virus on murine vascular

endothelial cells. J. Virol. 68, 3453–8.

Inoue, a, Choe, Y.K., Kim, B.S., 1994. Analysis of antibody responses to predominant linear epitopes of Theiler's murine encephalomyelitis virus. J. Virol. 68, 3324–3333. doi:10.1016/0165-5728(94)90367-0

Irwin, J.J., Shoichet, B.K., 2005. ZINC - A Free Database of Commercially Available Compounds for Virtual Screening 45, 177–182.

Jauka, T., Mutsvunguma, L., Boshoff, A., Edkins, A.L., Knox, C., 2010. Localisation of Theiler's murine encephalomyelitis virus protein 2C to the Golgi apparatus using antibodies generated against a peptide region. J. Virol. Methods 168, 162–169. doi:10.1016/j.jviromet.2010.05.009

Jiang, P., Liu, Y., Ma, H.-C., Paul, A. V., Wimmer, E., 2014a. Picornavirus morphogenesis. Microbiol. Mol. Biol. Rev. 78, 418–37. doi:10.1128/MMBR.00012-14

Jiang, P., Liu, Y., Ma, H.-C., Paul, A. V, Wimmer, E., 2014b. Picornavirus morphogenesis. Microbiol. Mol. Biol. Rev. 78, 418–37. doi:10.1128/MMBR.00012-14

Kilpatrick, D.R., Lipton, H.L., 1991. Predominant binding of Theiler's viruses to a 34-kilodalton receptor protein on susceptible cell lines. J. Virol. 65, 5244–5249.

Kim, B.S., Choe, Y.K., Crane, M.A., Jue, C.R., 1992. Identification and localization of a limited number of predominant conformation-independent antibody epitopes of Theiler's murine encephalomyelitus virus. Immunol. Lett. 31, 199–205. doi:10.1016/0165-2478(92)90146-F

Knox, C., Moffat, K., Ali, S., Ryan, M., Wileman, T., Wileman, T., 2005. Foot-and-mouth disease virus replication sites form next to the nucleus and close to the Golgi apparatus , but exclude marker proteins associated with host membrane compartments 687–696. doi:10.1099/vir.0.80208-0

Laskowski, R.A., Swindells, M.B., 2011. LigPlot + : Multiple Ligand À Protein Interaction Diagrams for Drug Discovery. J. Chem. Inf. Model. 51, 2778–2786.

Li, C., Wang, J.C.-Y., Taylor, M.W., Zlotnick, a., 2012. In Vitro Assembly of an Empty Picornavirus Capsid follows a Dodecahedral Path. J. Virol. 86, 13062–13069.

doi:10.1128/JVI.01033-12

Lipton, H.L., 1980. Persistent Theiler's murine encephalomyelitis virus infection in mie depends on plaque size. J. Gen. Virol. 46, 169–177.

Lipton, H.L., Friedmann, A., 1980. Purification of Theiler's murine encephalomyelitis virus and analysis of the structural virion polypeptides: correlation of the polypeptide profile with neurovirulence. J.Virol. 33, 1165–1172.

Liu, Q., Huang, X., Ku, Z., Wang, T., Liu, F., Cai, Y., Li, D., Leng, Q., Huang, Z., 2013. Characterization of enterovirus 71 capsids using subunit protein-specific polyclonal antibodies. J. Virol. Methods 187, 127–131. doi:10.1016/j.jviromet.2012.09.024

Luo, M., He, C., Toth, K.S., Zhang, C.X., Lipton, H.L., 1992. Three-dimensional structure of Theiler murine encephalomyelitis virus (BeAn strain). Proc Natl Acad Sci U.S.A 89, 2409–2413.

Macejak, D.G., Sarnow, P., 1992. Association of heat shock protein 70 with enterovirus capsid precursor P1 in infected human cells. J. Virol. 66, 1520–1527.

Mateo, R., Dı, A., Baranowski, E., Mateu, M.G., 2003. Complete Alanine Scanning of Intersubunit Interfaces in a Foot-and-Mouth Disease Virus Capsid Reveals Critical Contributions of Many Side Chains to Particle Stability and Viral Function * 278, 41019–41027. doi:10.1074/jbc.M304990200

Mateu, M.G., 1995. Antibody recognition of picornaviruses and escape from neutralization: A structural view. Virus Res. 38, 1–24. doi:10.1016/0168-1702(95)00048-U

Mateu, M.G., 1995. Antibody recognition of picornaviruses and escape from neutralization: a structural view. Virus Res. 38, 1–24. doi:10.1016/0168-1702(95)00048-U

Meloen Briaire, R.H.J., Woortmeyer, R.J., Van Zaane, D., 1983a. The main antigenic determinant detected by neutralizing monoclonal antibodies on the intact foot-and-mouth disease virus particle is absent from isolated VP1. J. Gen. Virol. 64, 1193–1198. doi:10.1099/0022-1317-64-5-1193

Meloen Briaire, R.H.J., Woortmeyer, R.J., Van Zaane, D., 1983b. The main antigenic

determinant detected by neutralizing monoclonal antibodies on the intact foot-and-mouth disease virus particle is absent from isolated VP1. J. Gen. Virol. 64, 1193–1198.

Monaghan, P., Gold, S., Simpson, J., Zhang, Z., Weinreb, P.H., Violette, S.M., Alexandersen, S., Jackson, T., 2005. The αvβ6 integrin receptor for Foot-and-mouth disease virus is expressed constitutively on the epithelial cells targeted in cattle. J. Gen. Virol. 86, 2769–2780. doi:10.1099/vir.0.81172-0

Morales, M., Tangermann, R.H., Wassilak, S.G.F., 2016. Progress Toward Polio Eradication - Worldwide, 2015-2016. MMWR. Morb. Mortal. Wkly. Rep. 65, 470–3. doi:10.15585/mmwr.mm6518a4

Morris, G.M., Huey, R., Lindstrom, W., Sanner, M.F., Belew, R.K., Goodsell, D.S., Olson, A.J., 2010. AutoDock4 and AutoDockTools4: Automated Docking with Selective Receptor Flexibility. J. Comput. Chem. 30, 2785–2791. doi:10.1002/jcc.21256.AutoDock4

Mullapudi, E., Nováček, J., Pálková, L., Kulich, P., Lindberg, A.M., van Kuppeveld, F.J.M., Plevka, P., 2016. Structure and genome release mechanism of human cardiovirus Saffold virus-3. J. Virol. 90, JVI.00746-16-. doi:10.1128/JVI.00746-16

Murray, L., Luke, G. a., Ryan, M.D., Wileman, T., Knox, C., 2009. Amino acid substitutions within the 2C coding sequence of Theiler's Murine Encephalomyelitis virus alter virus growth and affect protein distribution. Virus Res. 144, 74–82. doi:10.1016/j.virusres.2009.04.001

Nedellec, P., Vicart, P., Laurent-Winter, C., Martinat, C., Prevost, M.C., Brahic, M., 1998. Interaction of Theiler's virus with intermediate filaments of infected cells. J Virol 72, 9553–9560.

Nitayaphan, S., Toth, M.M., Roos, R.P., 1985. Neutralizing Monoclonal Antibodies to Theiler â€™s Murine Encephalomyelitis Viruses. Microbiology 53, 651–657.

Oberste, M.S., Maher, K., Kilpatrick, D.R., Pallansch, M.A., 1999. Molecular evolution of the human enteroviruses: correlation of serotype with VP1 sequence and application to picornavirus classification. J. Virol. 73, 1941–8.

Ohara, Y., Senkowski, A., Fu, J., Klaman, L., Goodall, J., Toth, M., Roos, R.P., 1988. Trypsin-

Sensitive Neutralization Site on VP1 of Theiler's Murine Encephalomyelitis virus 3527–3529.

Oleszak, E.L., Chang, J.R., Friedman, H., Katsetos, C.D., Platsoucas, C.D., 2004. Theiler ' s Virus Infection : a Model for Multiple Sclerosis. Society 17, 174–207. doi:10.1128/CMR.17.1.174

Pevear, D.C., Calenoff, M., Rozhon, E., Lipton, H.L., 1987. Analysis of the complete nucleotide sequence of the picornavirus Theiler's murine encephalomyelitis virus indicates that it is closely related to cardioviruses. J. Virol. 61, 1507–1516.

Reddi, H. V, Lipton, H.L., 2002. Heparan Sulfate Mediates Infection of High-Neurovirulence Theiler â€^{TM} s Viruses Heparan Sulfate Mediates Infection of High-Neurovirulence Theiler ' s Viruses 76, 8400–8407. doi:10.1128/JVI.76.16.8400

Rincón, V., Rodríguez-Huete, A., Mateu, M.G., 2015. Different Functional Sensitivity to Mutation at Intersubunit Interfaces Involved in Consecutive Stages of Foot-and-Mouth Disease Virus Assembly. J. Gen. Virol. doi:10.1099/vir.0.000187

Rombaut, B., Foriers, a., Boeye, a., 1991. In vitro assembly of poliovirus 14 S subunits: Identification of the assembly promoting activity of infected cell extracts. Virology 180, 781–787. doi:10.1016/0042-6822(91)90091-O

Ross, C., Knox, C., Bishop Tastan, O., 2017. Interacting motif networks located in hotspots associated with RNA release are conserved in Enterovirus capsids 1–15. doi:10.1002/1873-3468.12663

Ross, C., Upfold, N., Luke, G.A., Bishop, T.T., Knox, C., 2016. Subcellular localisation of Theiler's murine encephalomyelitis virus (TMEV) capsid subunit VP1 vis-á-vis host protein Hsp90. Virus Res. 222. doi:10.1016/j.virusres.2016.06.003

Ross, C., Upfold, N., Luke, G.A., Tastan, Ö., Knox, C., 2016. Subcellular localisation of Theiler ' s murine encephalomyelitis virus (TMEV) capsid subunit VP1 vis-á-vis host protein Hsp90. Virus Res. 222, 53–63. doi:10.1016/j.virusres.2016.06.003

Rossmann, M.G., Arnold, E., Erickson, J.W., Frankenberger, E. a, Griffith, J.P., Hecht, H.J., Johnson, J.E., Kamer, G., Luo, M., Mosser, a G., 1985. Structure of a human common cold

virus and functional relationship to other picornaviruses. Nature 317, 145–153. doi:10.1038/317145a0

Rossmann, M.G., Bella, J., Kolatkar, P.R., He, Y., Wimmer, E., Kuhn, R.J., Baker, T.S., 2000. Cell Recognition and Entry by Rhino- and Enteroviruses. Virology 269, 239–247. doi:10.1006/viro.2000.0258

Shah, A.H., Lipton, H.L., 2002. Low-neurovirulence Theiler's viruses use sialic acid moieties on N-linked oligosaccharide structures for attachment. Virology 304, 443–450. doi:10.1006/viro.2002.1735

Shieh, J.T.C., Bergelson, J.M., 2002. Interaction with Decay-Accelerating Factor Facilitates Coxsackievirus B Infection of Polarized Epithelial Cells Interaction with Decay-Accelerating Factor Facilitates Coxsackievirus B Infection of Polarized Epithelial Cells. J. Virol. 76, 1–8. doi:10.1128/JVI.76.18.9474

Stanway, G., 1990. Structure, function and evolution of picornaviruses. J. Gen. Virol. 71, 2483–2501. doi:10.1099/0022-1317-71-11-2483

Staunton, D.E., Merluzzi, V.J., Rothlein, R., Barton, R., Marlin, S.D., Springer, T. a, 1989. A cell adhesion molecule, ICAM-1, is the major surface receptor for rhinoviruses. Cell 56, 849–53. doi:10.1016/0092-8674(89)90689-2

Tan, C.-S., Cardosa, M.J., 2007. High-titred neutralizing antibodies to human enterovirus 71 preferentially bind to the N-terminal portion of the capsid protein VP1. Arch. Virol. 152, 1069–73. doi:10.1007/s00705-007-0941-1

Tsunoda, I., Libbey, J.E., Fujinami, R.S., 2010. Theiler's murine encephalomyelitis virus attachment to the gastrointestinal tract is associated with sialic acid binding. J. Neurovirol. 15, 81–89. doi:10.1080/13550280802380563.Theiler

Tuthill, T.J., Groppelli, E., Hogle, J.M., Rowlands, D.J., 2010a. Picornaviruses, in: Johnson, J.E. (Ed.), Cell Entry by Non-Enveloped Viruses. Springer Berlin Heidelberg, Berlin, Heidelberg, pp. 43–89. doi:10.1007/82_2010_37

Tuthill, T.J., Groppelli, E., Hogle, J.M., Rowlands, D.J., 2010b. Picornaviruses. curr Top Microbiol Immunol. 343, 43–89. doi:10.1007/82_2010_37

Varrasso, A., Drummer, H.E., Huang, J. a, Stevenson, R. a, Ficorilli, N., Studdert, M.J., Hartley, C. a, 2001. Sequence conservation and antigenic variation of the structural proteins of equine rhinitis A virus. J. Virol. 75, 10550–10556. doi:10.1128/jvi.75.21.10550-10556.2001

Westerhuis, B.M., Benschop, K.S.M., Koen, G., Claassen, Y.B., Wagner, K., Bakker, A.Q., Wolthers, K.C., Beaumont, T., 2015. Human Memory B Cells Producing Potent Cross-Neutralizing Antibodies against Human Parechovirus : Implications for Prevalence , Treatment , and Diagnosis. J. Virol. 89, 7457–7464. doi:10.1128/JVI.01079-15

Wu, C.N., Lin, Y.C., Fann, C., Liao, N.S., Shih, S.R., Ho, M.S., 2001. Protection against lethal enterovirus 71 infection in newborn mice by passive immunization with subunit VP1 vaccines and inactivated virus. Vaccine 20, 895–904. doi:10.1016/S0264-410X(01)00385-1

Wu, X., Li, X., Zhang, Q., Wulin, S., Bai, X., Zhang, T., Wang, Y., Liu, M., Zhang, Y., 2015. Identification of a conserved B-cell epitope on duck hepatitis a type 1 virus VP1 proteine0118041. PLoS One 10, 1–11. doi:10.1371/journal.pone.0118041

Wychowski, C., Werf, S. Van Der, Girard, M., 1985. Nuclear localization of poliovirus capsid polypeptide VP1 expressed as a fusion protein with and analysis 37, 63–71.

Yang, D., Zhang, C., Zhao, L., Zhou, G., Wang, H., Yu, L., 2011. Identification of a conserved linear epitope on the VP1 protein of serotype O foot-and-mouth disease virus by neutralising monoclonal antibody 8E8. Virus Res. 155, 291–299. doi:10.1016/j.virusres.2010.10.024

Zhang, J., Dong, M., Jiang, B., Dai, X., Meng, J., 2012. Antigenic characteristics of the complete and truncated capsid protein VP1 of enterovirus 71. Virus Res. 167, 337–342. doi:10.1016/j.virusres.2012.05.019

Zhou, L., Luo, Y., Wu, Y., Tsao, J., Luo, M., 2000. Sialylation of the host receptor may modulate entry of demyelinating persistent Theiler's virus. J Virol 74, 1477–1485. doi:10.1128/JVI.74.3.1477-1485.2000

Zurbriggen, A., Fujinami, R.S., 1989. A Neutralization-Resistant Theiler â€™ s Virus Variant Produces an Altered Disease Pattern in the Mouse Central Nervous System 63, 1505–1513.

Zurbriggen, A., Hogle, J.M., Fujinami, R.S., 1989. Alteration of Amino Acid 101 Within Capsid

Protein VP-1 Changes the Pathogenicity of Theiler's Murine Encephalomyelitis Virus. J. Exp. Med. 170, 2037–2049.

Table 1. Primers used to generate plasmids expressing VP1 truncates

Primer	Primer sequence
NUVP1F	5' AAA GGA TCC GGA ATT GAC AAT GCT G 3'
NUVP1R	5' AAA GTC GAC TCA CTC AAG CTC AAG AAT G 3'
NU1-112R	5' AAA GTC GAC TCA CTG TTT GGT CAT GAT GG 3'
NU1-195R	5' AAA GTC GAC TCA CAG AGG GGA ATT GTA AGG 3'
NU1-221R	5' AAA GTC GAC TCA ATC CGA CGT AGG AGC AAC 3'

NU159-276F	5’ AAA GGA TCC GTC ACT GAC CAG CTG ATC 3’
NU159-276R	5’ AAA GTC GAC TCA CTC AAG CTC AAG AAT G 3’

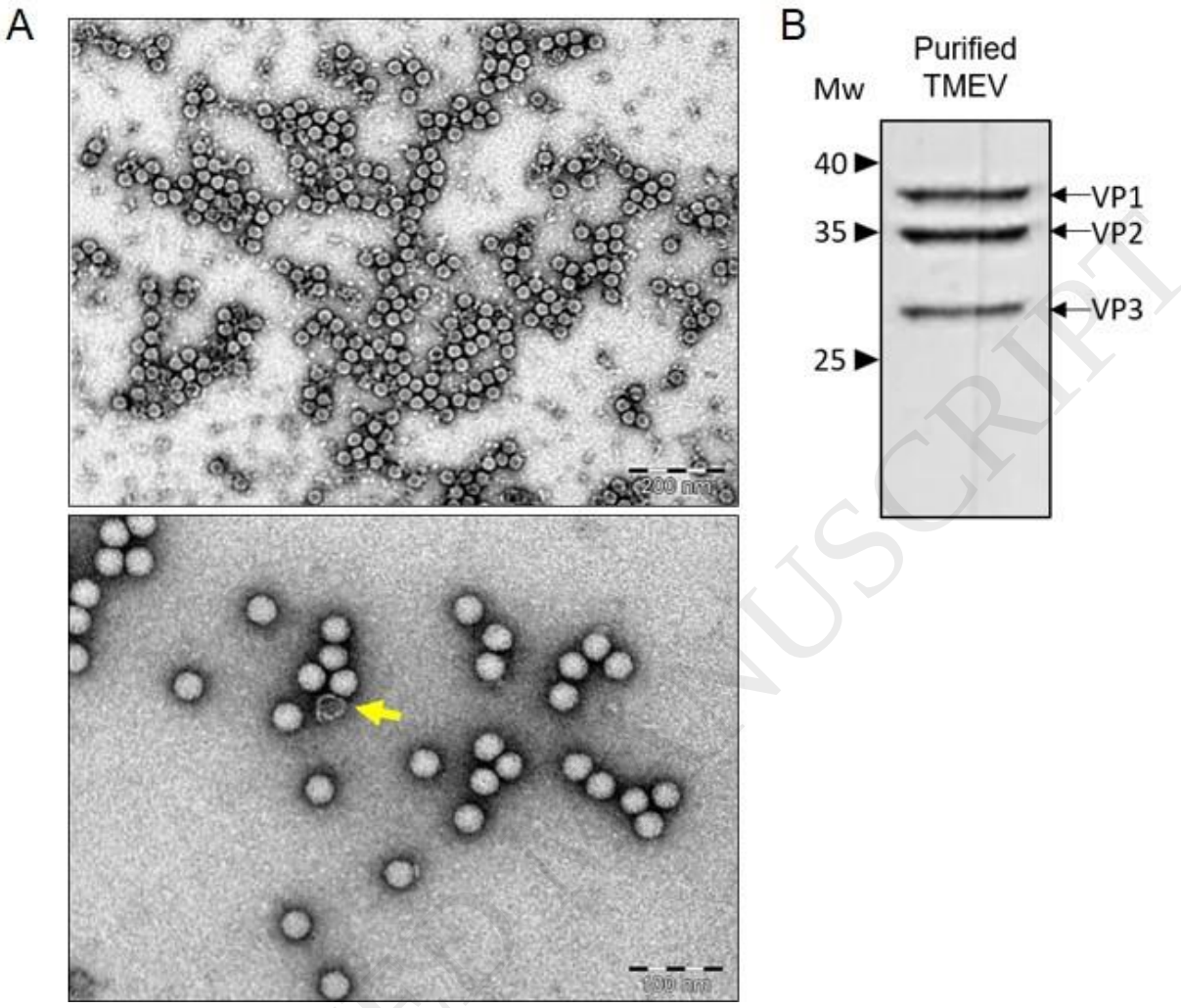

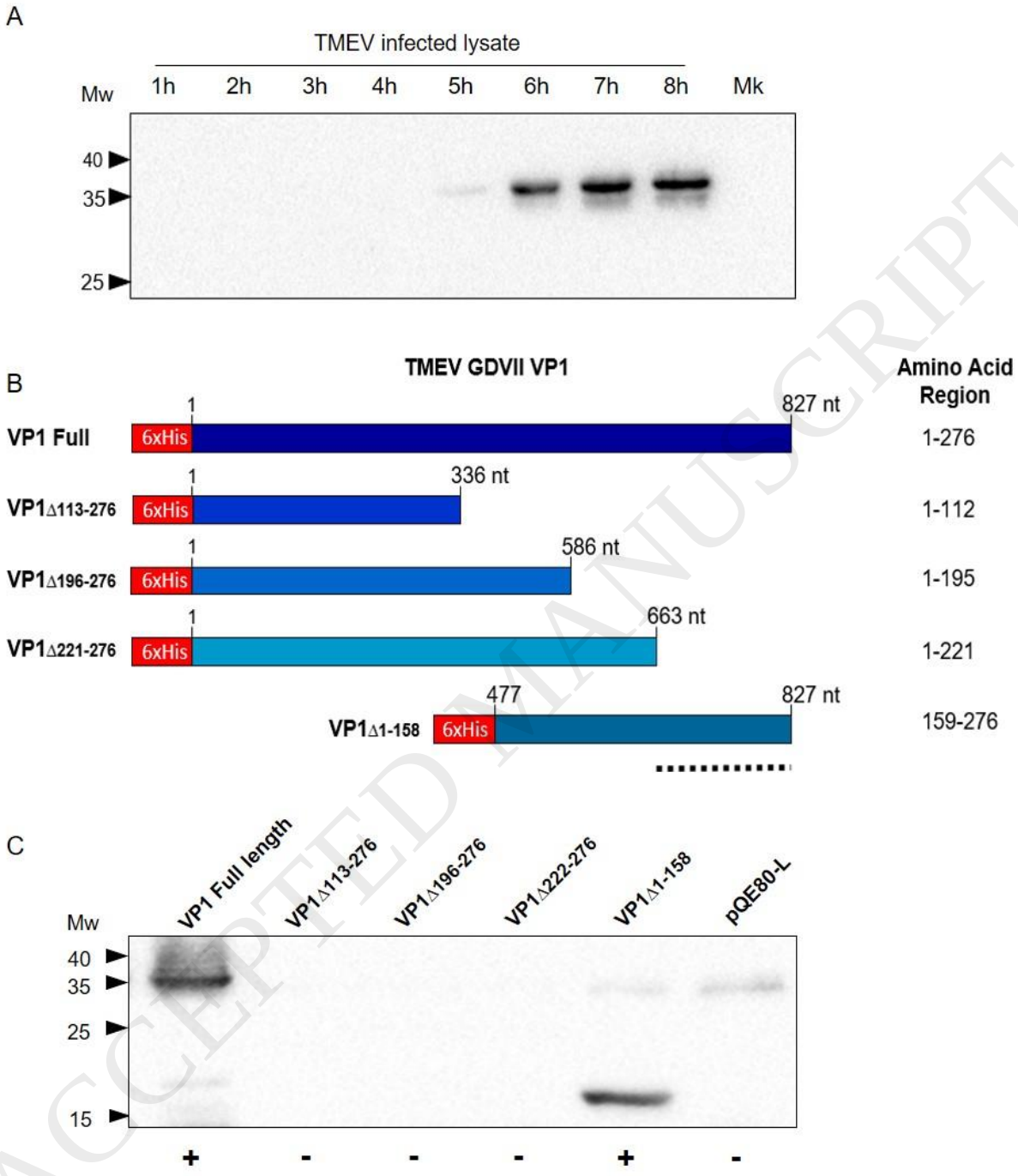

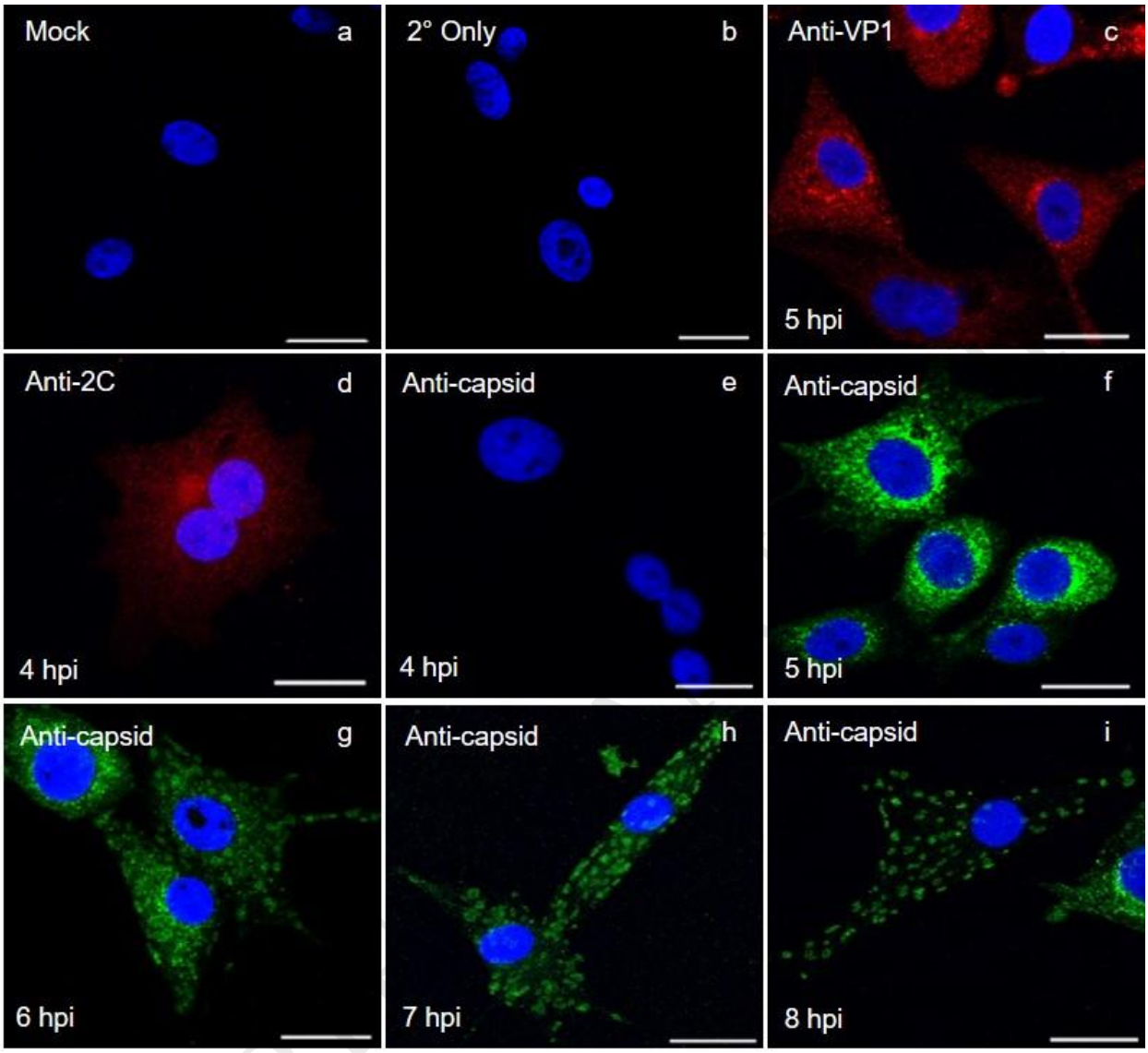

A

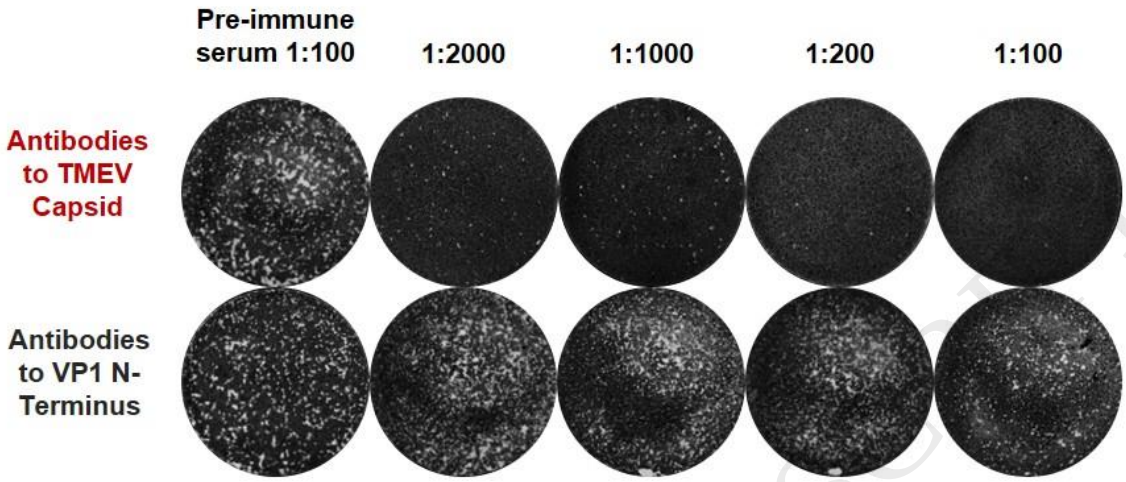

B

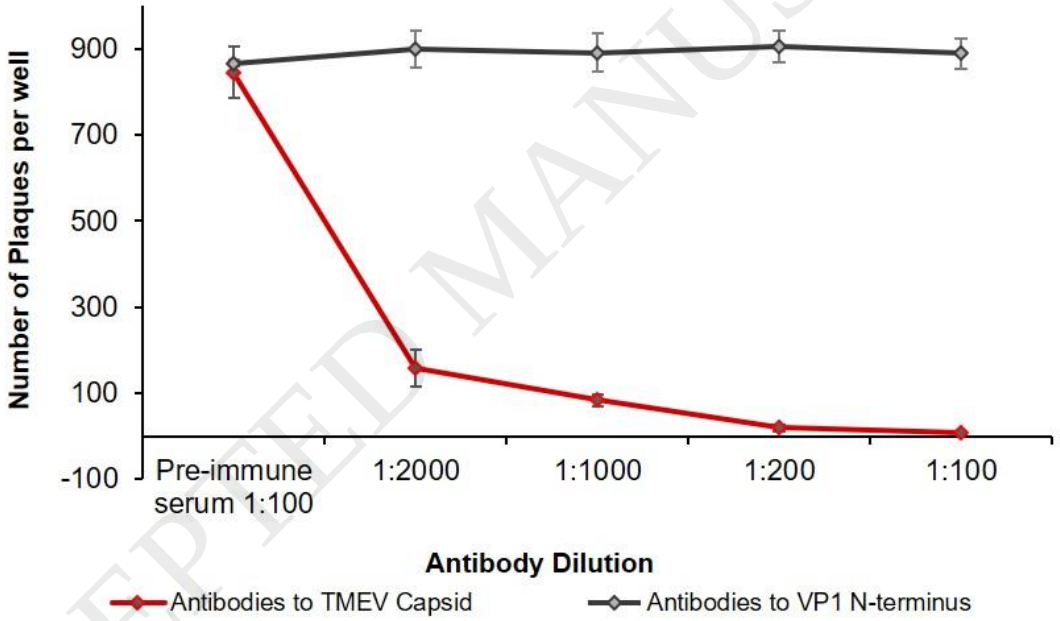

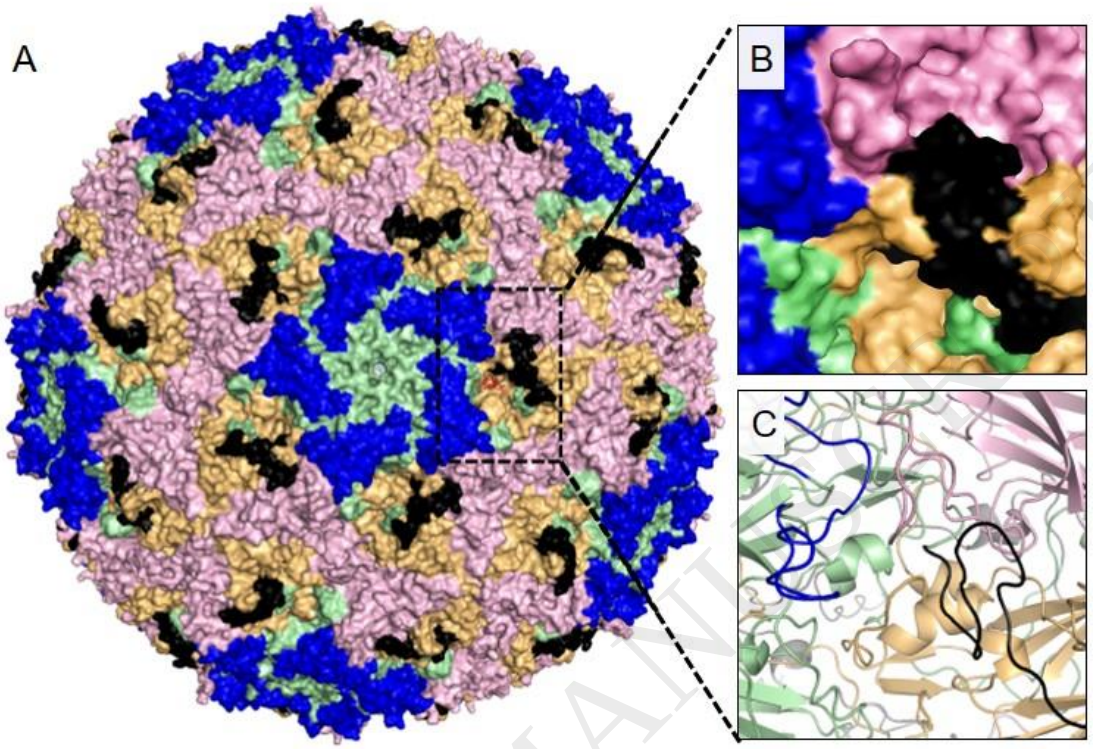

A